Proceedings of the EuroGNC 2013, 2nd CEAS Specialist Conference
on Guidance, Navigation & Control, Delft University of Technology,
Delft, The Netherlands, April 10-12, 2013

ThCT3.4

Gyro bias estimation using a dual instrument configuration

Marcel Ruizenaar, Elwin van der Hall, and Martin Weiss

Abstract An innovative method is proposed for the estimation of inertial measurement biases. This method, that we call DriftLess^{TM}, is based on fusing the data from two sets of inertial measurement sensors that are displaced with respect to each other by a known angle. By varying the relative position of the sensors according to a predefined pattern, it is possible to acquire sufficient measurement data in order to estimate the biases of both sensors. The method was validated and tested in a laboratory installation and a numerical sensitivity study was conducted in order to evaluate the feasibility of the method for more realistic settings.

1 Introduction

The interest in robust autonomous navigation systems has grown steadily in the last years and has been driven both from the increasing number of applications and from the awareness of the inherent limits of the satellite-based navigation systems such as GPS. Autonomous inertial navigation remains the only navigation solution that cannot be intentionally or unintentionally disturbed by external factors. It is however limited by the presence of measurement errors from the inertial measurement instruments: gyros and accelerometers. The measurement errors we are interested in are the systematic errors and not the random errors. The latter is transformed in random walk after integration. There are three main types of systematic errors that affect inertial measurements: bias errors, scale factor errors and cross-coupling (or misalignment) errors. Bias errors have essentially four components: fixed errors that are characteristic to the instrument and are constant, temperature-dependent er-

Marcel Ruizenaar, Elwin van der Hall
TNO Organization, The Hague, Netherlands, e-mail: marcel.ruizenaar@tno.nl, elwin.vanderhall@tno.nl

Martin Weiss
TNO Organization, Rijswijk, Netherlands, e-mail: martin.weiss@tno.nl

1

rors, run-to-run errors that are constant during each single run, and in-run errors that may vary during the run. The fixed and temperature-dependent errors are typically compensated partially by calibration. Run-to-run errors are compensated through alignment, but this is not always possible. In-run errors may only be mitigated by integrating different measurement instruments in a sensor fusing scheme. Bias errors are in most practical cases the dominant errors. Therefore, we will concentrate here on the compensation of bias errors of inertial instruments.

Commonly, the bias error is decomposed in two components: static bias and dynamic bias. Static bias errors are constant during a run and consist mainly of the run-to-run bias errors and residuals of fixed bias errors after the calibration process. Dynamic bias errors may vary during a run over periods in the order of minutes or more and consist mainly of in-run bias errors and residuals of temperature dependent errors after the calibration process. An effective procedure to compensate bias errors needs to take into consideration both static and dynamic bias errors and therefore has to be performed repeatedly during the traversed trajectory.

As the navigation solution is obtained by integrating the sensor measurements, bias errors lead to growing position and orientation errors. This is especially true for low cost equipment. Here, measures to reduce bias errors have a relative large impact on the cost. Because the growth of these errors can indeed make the navigation solution unacceptable in a very short time, it is essential to correct them. Therefore much research is being done on this topic. As explained before, the bias errors that cannot be corrected by calibration are addressed by alignment or by sensor fusion. In either case, the results of different measurements are used to estimate and correct bias errors. A large variety of methods are used in practice and many variations and improvements can be found in the literature. One of the most popular methods is the integration of an inertial navigation system (INS) with satellite navigation, leading to integrated INS/GPS systems of various types. However, many other sensors can be used to correct inertial measurements, such as magnetometers and altimeters. A special category of sensors used for correcting or improving inertial navigation are imaging sensors, typically used in conjunction with terrain matching, or other localization techniques. For an overview of these techniques we refer to [4].

The technique proposed in this paper is similar to other known techniques in the sense that it combines the output of two instruments in order to improve the measurement accuracy of both. The difference is that the two sensors of the same type are displaced with respect to each other in a controlled manner that allows us to accurately estimate and compensate for the bias errors. The estimation can be done during operation, which is one of the major advantages. If the other systematic errors are properly calibrated, theoretically only white noise remains after compensation for the estimated biases. In this paper we explain the method as applied to gyro bias correction, but the method is equally applicable to accelerometers and other sensors that measure a vectorial quantity (such as, magnetometers) [8]. A similar method for bias estimation using identical sensors is presented in [9], where a static configuration of twelve accelerometers is used to estimate the bias of gyros. In contrast, our method uses a dynamic configuration of only two gyros to achieve the same goal.

The structure of the paper is as follows. In Section 2 we present the theoretical basis of the DriftLess$^{\text{TM}}$ concept. The results of a study based on digital simulation experiments are presented in Section 3. Section 4 gives a description of the experimental set-up, the calibration of the set-up and presents experimental results. Finally, conclusions and ideas for future work are relegated to Section 5.

2 Theoretical description of the DriftLess$^{\text{TM}}$ concept

The bias is a (largely) constant error that affects the measurements of every inertial sensor and it is independent of the measured quantity. Biases can be split into static and dynamic biases. The static component, called the fixed bias, is constant throughout a run. The dynamic component, also refered to as bias instability, varies slowly during a run over periods in the order of a minute or more due, for example, to uncompensated temperature variations and inherent instability of the sensor. Typically, the dynamic bias is 10% of the static bias. Although there are many other sources of errors (see e.g. [4]), the bias error of gyros is dominating the error budget of the navigation solution. We therefore use gyros as a concrete example for explaining the DriftLess$^{\text{TM}}$ concept.

To illustrate the instability of the bias, the averaged output of 6 low-cost MEMS gyros has been plotted as a function of time in Figure 1. During measuring, the sensors were held stationary and at nearly constant temperature (within 0.5 °C). The measurement time was approx. 14 hours. The plot clearly shows that if the bias was initially zeroed after some calibration procedure, the bias could have deviated to almost 1000 deg/hr after several hours of operation.

The general principle of the DriftLess$^{\text{TM}}$ method is presented graphically in Figure 2. We will explain this scheme and the listed parameters by stepwise introducing our method. The concept involves two sets of sensors. Each set is a triad of, preferably orthogonal, gyroscopes. The two sets of sensors S_1 and S_2 are mounted on rotatable platforms. They are actuated by the motors M_1 and M_2 that rotate the two sets of sensors back and forth using a periodic scheme around two different axes.

Let the measured vectorial quantity $\mathbf{x}$ represent the angular rate of a common body frame relative to the inertial frame and let $\mathbf{y_1}$ and $\mathbf{y_2}$ be the two measurement sets provided by the two sensor sets. If all other systematic errors are assumed to be calibrated, then $\mathbf{x}$, $\mathbf{y_1}$ and $\mathbf{y_2}$ are related by:

$$\begin{aligned} \mathbf{y}_1 &= R_1^T \mathbf{x} + \mathbf{b}_1 + \omega_1 + \mathbf{n_1} \\ \mathbf{y}_2 &= R_2^T \mathbf{x} + \mathbf{b}_2 + \omega_2 + \mathbf{n_2} \end{aligned} \tag{1}$$

where R_1 and R_2 are the rotation matrices corresponding to the attitude of the two platforms with respect to the body frame. ω_1 and ω_2 are the angular rates of the two platforms with respect to the body frame. $\mathbf{b}_1$ and $\mathbf{b}_2$ are the measurement biases of the two sensor sets, and $\mathbf{n_1}$ and $\mathbf{n_2}$ are the random noise components of the measurement errors.
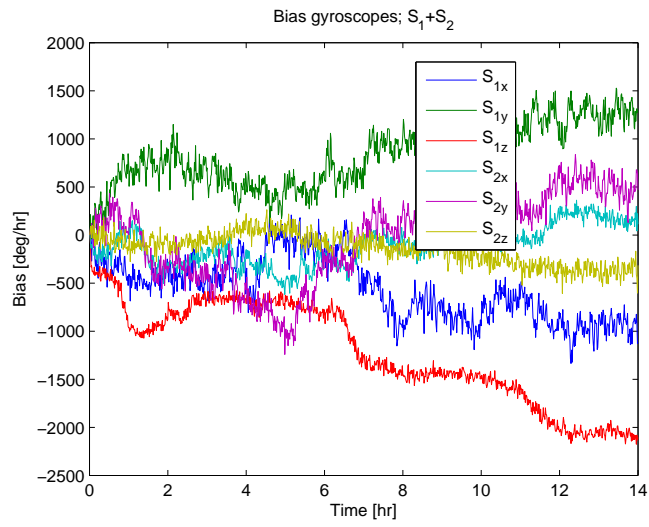
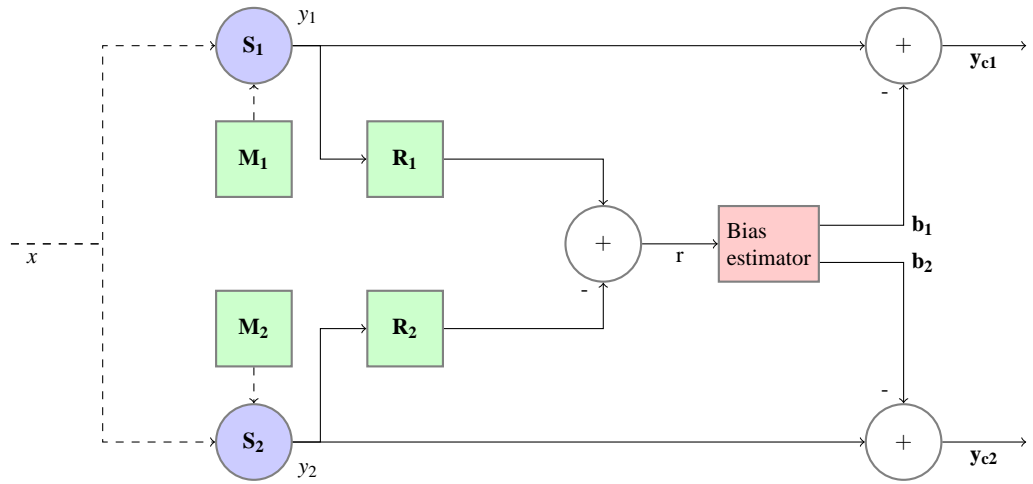**Fig. 1** Evolution of six different bias estimates during a 14h experiment.

Fig. 2 Schematic representation of the DriftLess$^{\text{TM}}$ concept.

Since the error model of the inertial sensors is quite complicated, we assume here that the biases $\mathbf{b}_i$ are constant during the time period of the rotation scheme and that the random noises $\mathbf{n_i}$ are white noise signals. According to the diagram in Figure 2, the two measurement sets are used to compute a residual signal $\mathbf{r}$.

$$\begin{aligned}\mathbf{r} &= R_1\mathbf{y}_1 - R_2\mathbf{y}_2\\ &= R_1(\mathbf{b}_1 + \omega_1) - R_2(\mathbf{b}_2 + \omega_2) + (R_1\mathbf{n_1} - R_2\mathbf{n_2})\end{aligned} \tag{2}$$

The residual $\mathbf{r}$ is independent of the input quantity $\mathbf{x}$. This is a very advantageous characteristic of the method, making it applicable in dynamic situations. The idea is to use the residual for estimating the bias errors of the sensors. The estimated biases can then be subtracted from the measurements to yield the corrected measurements y_{1c} and y_{2c}. Of course, using equation (2) instead of the raw measurement equations (1) we cannot "solve" both for $\mathbf{b}_1$ and $\mathbf{b_2}$ given $\mathbf{r}$. However, the idea is to collect multiple residual measurements for different relative positions of the sensor sets and use these to estimate the bias errors. By judiciously choosing the angular displacement of the sensor sets with respect to the body frame, the biases become observable.

For simplicity, we choose to perform the measurements with the two platforms at rest with respect to the body frame, that is $\omega_1=\omega_2=0$. Furthermore, each of the sensor sets is alternating between two predefined positions. According to the simulation results [10], it is preferable that the rotation axes are orthogonal and the angular positions are ±90deg. Essentially, the rotation matrix R_1 at the time of the measurement may take two values that we denote R_1^{+90} and R_1^{-90}, and similarly R_2 takes the values R_2^{+90} and R_2^{-90}. The motion of both sensor sets follows the typical scheme illustrated in Figure 3 and the measurements of the residuals is taken only when both sets are at rest with respect to the body frame.

The residual measurements can be modelled by the following discrete time system

$$\begin{aligned}\mathbf{x}_{k+1} &= A\mathbf{x}_k + \mathbf{w}_k\\ \mathbf{r}_k &= H_k\mathbf{x}_k + \mathbf{v}_k\end{aligned} \tag{3}$$

where

$$\mathbf{x}_k = \begin{bmatrix}\mathbf{b}_1\\\mathbf{b}_2\end{bmatrix}, A = \begin{bmatrix}I&\\&I\end{bmatrix} \tag{4}$$

and

$$H_k = \begin{cases}\begin{bmatrix}R_1^{+90}&-R_2^{+90}\end{bmatrix}, & k=4n\\\begin{bmatrix}R_1^{+90}&-R_2^{-90}\end{bmatrix}, & k=4n+1\\\begin{bmatrix}R_1^{-90}&-R_2^{-90}\end{bmatrix}, & k=4n+2\\\begin{bmatrix}R_1^{-90}&-R_2^{+90}\end{bmatrix}, & k=4n+3\end{cases} \tag{5}$$

Here $\mathbf{w}_k$ represents the process noise that models the bias instability, whereas $\mathbf{v}_k$ represents the measurement noise terms in equation (2). As usual they are assumed to be delta-correlated, discrete signals.

Using a Kalman filter based on this model, it is possible to estimate the two biases $\mathbf{b}_1$ and $\mathbf{b}_2$ based on the residuals $\mathbf{r}_k$ and use them to correct the inertial measurements. The basics of Kalman filtering are well described in literature and falls out of the scope of this paper. For further reading, we refer to [7],[5],[4]. The Kalman filter recursion formulas we used for our particular case are:

$$S_{k+1} = R_{k+1} + H_{k+1}(P_k + Q_k)H_{k+1}^T$$
$$W_{k+1} = (P_k + Q_k)H_{k+1}^T S_{k+1}^{-1}$$
$$P_{k+1} = (I - W_{k+1}H_{k+1})(P_k + Q_k)$$
$$\hat{\mathbf{x}}_{k+1} = \hat{\mathbf{x}}_k + W_{k+1}(\mathbf{r}_{k+1} - H_{k+1}\hat{\mathbf{x}}_k)$$

System matrix A is the identity matrix and has been left out of the equations. Initial values $\hat{\mathbf{x}}_0$ and P_0 have been chosen, and $Q_k = E[\mathbf{w}_k^T \mathbf{w}_k]$ and $R_k = E[\mathbf{v}_k^T \mathbf{v}_k]$ are the variance matrices of the process, and the measurement noise terms respectively. Further, P_k is the state covariance matrix and W_k is the Kalman gain.
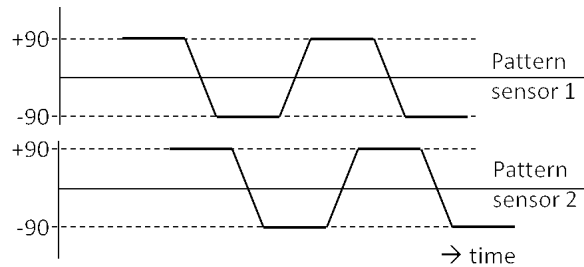

Fig. 3 Angular displacement for the two sensor sets.

Commonly the performance of inertial sensors is analysed with the Allan variance (AV). This time domain characteristic of the accuracy of a sensor was first introduced to analyse the precision of oscillators for time measurements [1], but has been widely applied to characterize the accuracy of inertial sensors [3][11]. We will use this characteristic to illustrate the improvement realized using the DriftLess[TM] concept with respect to the raw sensor measurements.

For completeness, we recall here the definition of the AV as we use it here. Assume we have N measurement samples of the angular velocity ω_i, measured with a sampling time τ_o and we divide the samples into clusters of size M. The time period corresponding to a single cluster is $\tau = M\tau_o$ and is called the correlation time or integration time. The average for each cluster is denoted by

$$\bar{\omega}_k(\tau) = \frac{1}{M}\sum_{i=1}^{M}\omega_{kM+i}, \, k = 0, 1, \ldots, K-1, K = \left\lfloor \frac{N}{M} \right\rfloor$$

Then the Allan variance is computed as

$$\sigma_\omega^2(\tau) = \frac{1}{2K} \sum_{k=0}^{K-1} (\bar{\omega}_{k+1}(\tau) - \bar{\omega}_k(\tau))^2$$

The AV can be seen as a measure of the stability of the bias for a given integration time. It tells us how good a measured average cluster value predicts the average value of the succeeding cluster. A typical plot of the Allan variance as a function of the integration time is shown in Figure 5. The red lines are Allan variances of actual MEMS gyro measurements. In general, for MEMS gyros, the plot has some typical features. Going from low integration times (left side of the plot) to larger integration times, the plot decreases almost linearly. This is due to the white noise on the output of the sensor. After some point the plot increases, typically at large integration times. This is due to the low frequent, non-white noise on the output of the sensor (the fluctuating bias). The minimum in the plot corresponds to the integration time at which the best bias stability can be expected. For MEMS sensors this integration time is typically in the order of 100 s.

3 Simulation results

For further design improvements a numerical model of the experimental set-up has been built. With this model a sensitivity analysis has been performed to determine the influence of certain design parameters on the accuracy of the bias estimation.

Firstly, we tested the influence of the rotation angle applied by the motors on the sensors. By varying the angle between 0 and ± 90 deg, we determined that the bias estimation was most accurate if the motors turned ± 90 deg. In theory any angle greater than 0 renders all biases observable but due to noise and numerical inaccuracies the accuracy degrades as the rotation angle is smaller.

Secondly, we checked the influence of angle misalignments. The two sensors are mounted orthogonally and their relative attitude with respect to the body frame needs to be accurately known. Any misalignment results in an additional term, that depends on the angular velocity, entering the Kalman filter. This results in an error in some of the estimated biases, which depends on the input angular rate in a non-linear way. Beside constant misalignments, dynamic offsets may also occur due to, for example, motor overshoots. The effects are the same as in the case of constant misalignments but the effects are mitigated for the two bias estimations on the rotational axis due to carouselling.

Thirdly the Kalman filter bandwidth was varied. In this respect we note that the Kalman filter has the characteristics of a low-pass filter for our application and that the sensors rotate between two positions periodically with a certain frequency. It is essential that this frequency is filtered away sufficiently, otherwise the bias estimation accuracy deteriorates. The rotational frequency is limited by the required standstill time of both sensors during the actual measurement. This standstill time may not be too long, because three different positions are necessary within the Kalman filter bandwidth to obtain full observability of the biases. Too short a standstill time

is not possible, because the bias changes slowly but continuously. During standstill sufficient convergence has to be achieved to keep up with these changes.

The noise power and sample frequency were also varied. As expected the accuracy of the bias estimate is linearly dependent on the power of the noise of the measurements. Because the bias instability is a very low frequency phenomenon, a low measurement frequency can be used without adverse effects.

Lastly some errors that may occur with the AD-converter have been modelled such as missing bins and non-linearities. These errors turned out to have little effect on the bias estimation accuracy.

The simulation results for a 14 hour simulation are given in Figure 4. In this figure, simulated and estimated bias are plotted.

An interesting property of the concept is that if the set-up is at rest (i.e., no input angular rate), it does not matter if the rotation matrices used in the calculations correspond to the actual sensor positions. As $\mathbf{x} = 0$, any erroneously used R_i in equation (1) does not introduce an error in the residual $\mathbf{r}$, input to the Kalman filter (equation (2)). We used this property to measure the output of two sets of MEMS gyros that were at rest with respect to our laboratory set-up (i.e., no rotation of the common body and no rotation of the sensors). The total measurement time was 14 hr. We calculated the Allan variance of these measurements and they are plotted in Figure 5 (for clarity, only the plots of three gyros are shown of six available). Also we ran our DriftLess^{TM} algorithm using these measured gyro signals as input and calculated the biases. After compensating for the biases, we calculated the AV again and plotted the results (of the three gyros) in the same figure. From these plots we observe that the concept performs as expected.
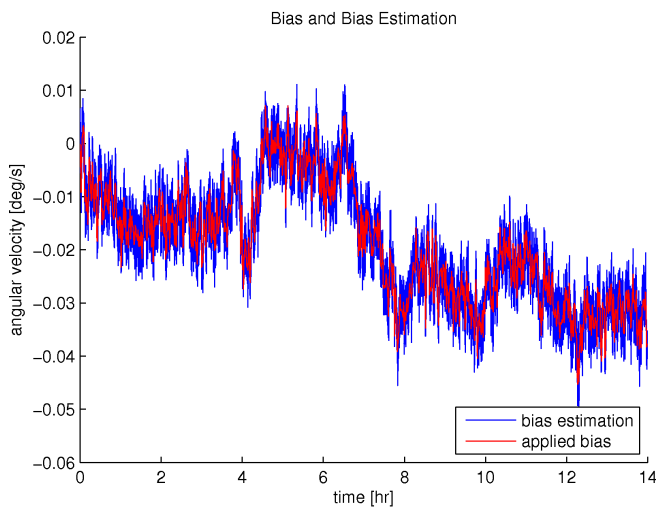

Fig. 4 14 hour run bias estimation. The red line is the bias, the blue line the estimate of this bias.
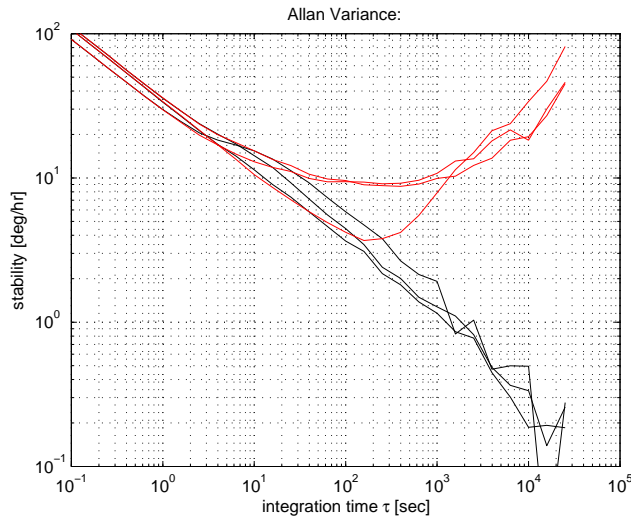
Allan Variance:

Fig. 5 Allan variance of a 14 hour experiment. The red lines are the Allan variances of the uncorrected biases of a single gyro triad and the black lines are the Allan variances of the sensors corrected with our DriftLess^{TM} concept

4 Experimental set-up

The experimental set-up used to validate and test the DriftLess^{TM} concept is represented in Figure 6. Figure 7 is a photo of the actual implementation. For the two sets of sensors S_1 and S_2 we used the MPU6050 3-axis MEMS gyro of Invensense [6]. The sensors are sampled with a frequency of 100 Hz. The gyro noise floor of the sensors is typically 0.005 deg/rt(Hz), yielding a residual noise covariance equivalent to approximately 2×0.052 deg^2/s^2. The two sensor chips are each placed on their own rotatable printed circuit board (PCB) together with some interfacing electronics. The PCBs are rotated with a driving mechanism based on small piezo-elements, desifned by the Danish company PCBmotor [2]. On the right side of the box in Figure 7, a third PCB is mounted containing all the necessary driving and interfacing electronics, and a USB interface to connect to a computer. End stops are used on the sensor PCBs to limit the rotation between two fixed angular positions (approximately ± 90 degrees).

In general, a calibration procedure has to be performed to find the coefficients of a calibration matrix C for each sensor, containing all information about scaling factors (including the analog to digital converter gain), misalignment, and cross-coupling coefficients. Specifically for our DriftLess^{TM} concept, another calibration procedure is required to find a rotation matrix T for all individual angular positions. These two matrices C and T can be combined into a single matrix M which replaces the rotation matrices R in equation (1). However, since M is no longer a rotation matrix, M^T has to be replaced with M^{-1}. Instead of using two separate calibration
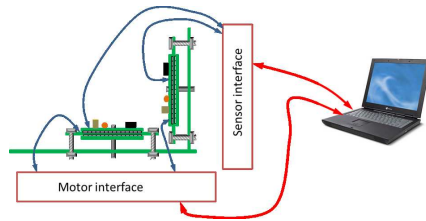
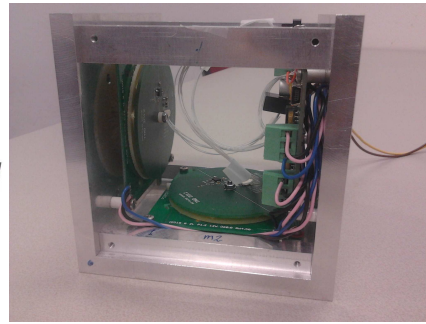**Fig. 6** Scheme of the laboratory set-up used for testing the DriftLess^{TM} concept.

Fig. 7 Photo of the actual experimental installation used to test Driftless^{TM}.

procedures, our calibration procedure finds all coefficients of the matrix *M* for each of the individual angular positions. For the calibration, we used an accurate pan/tilt unit providing a known angular rate of 50 deg/s to the gyros.

The box was assembled in such a way that all sides of the box are orthogonal to within 0.05 deg. First both sensors were placed in their -90-position. The box was rotated back and forth to known angular positions with the same angular rate. During this 1 minute lasting process, gyro measurements were recorded. This process was repeated with the box placed in its XY-orientation, YZ-orientation and XZ-orientation. As an example, Figure 8 shows the actual output of the S_1 gyro. The top of the large square wave outputted by the z-axis gyro of S_1 corresponds to the positive angular rate of 50 deg/s and the bottom to -50 deg/s. The smaller square waves outputted by the x- and y-axes are due to the misalignment of these axes with respect to the z-axis. Measuring the average top-top values of the square waves provides us with all necessary information to obtain the coefficients of the matrices *M* for both sensors in their -90-position. Then the sensors were placed in their +90-positions and the process was repeated to find the matrices M for the sensors in their +90-position.

The outputs of the gyros ($\mathbf{y}_{c1}$ and $\mathbf{y}_{c2}$ in Figure 2), after bias correction by DriftLess^{TM} and after compensation for Earth rotation, were used to continuously update a rotation matrix R_{be} representing the attitude of the "DriftLess^{TM} box" with respect to the local Earth navigation frame. The experimental set-up was placed on the same pan-tilt unit that was used for the calibration procedure. With this unit we were able to test the DriftLess^{TM} concept in a dynamical situation. Random but known angular patterns were used to drive the pan/tilt unit. As the actual pan/tilt angles are known, we could compare them to the attitude information derived from the R_{be} rotation matrix. Figure 9 shows the difference in attitude using our DriftLess^{TM} system and without using DriftLess^{TM}. As can be seen, the attitude drift without using DriftLess^{TM} is in the order of 250 deg/hr. After correction with DriftLess^{TM}, the remaining drift is in the order of 20 deg/hr.
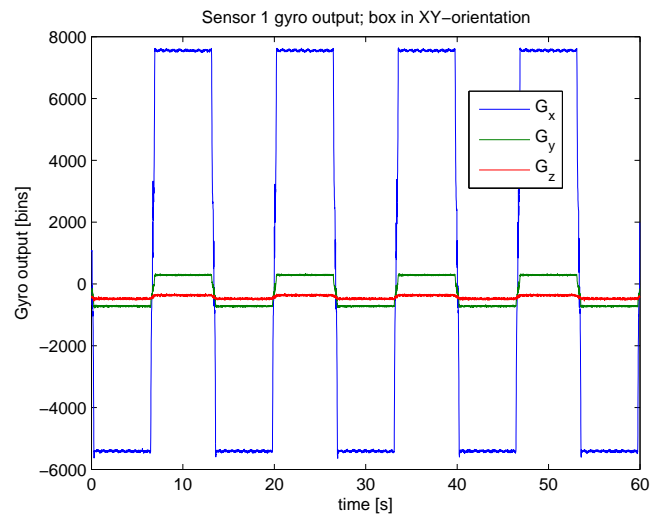
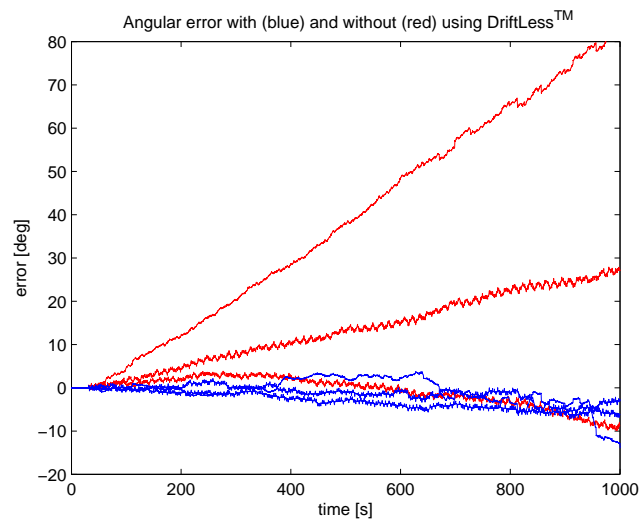**Fig. 8** The gyroscope signals during a calibration process.

Fig. 9 The angular errors of a gyroscope. The red lines are without applying Driftless[TM] and the blue lines are with Driftless[TM] applied.

5 Conclusions and further work

We have presented in this paper an innovative method for bias estimation of inertial sensors. The principle of the method is to combine measurements from two sets of INS instruments that are displaced with respect to each other according to a controlled pattern. The method was tested on gyro sensors in an experimental setting and also in a few digital simulation studies. The results presented here indicate that the method promises to be very effective and may allow high performance navigation results using cheaper sensor instrumentation.

Further work will concentrate on fault detection and isolation algorithms to allow this approach to work under difficult terrain conditions and under considerable stress. In parallel, work is going on in order to miniaturize the installation in order to allow application in a large variety of situations such as unmanned ground or air vehicles, guided weapons, and personal (indoor) navigation.

References

1. D.W. Allan. Statistics of atomic frequency standards. *Proceedings of the IEEE*, 54(2):221 – 230, feb. 1966.
2. PCBMotor ApS. http://pcbmotor.com/. Web page.
3. N. El-Sheimy, Haiying Hou, and Xiaoji Niu. Analysis and modeling of inertial sensors using allan variance. *Instrumentation and Measurement, IEEE Transactions on*, 57(1):140 –149, jan. 2008.
4. P.D. Groves. *Principles of GNSS, inertial, and multi-sensor integrated navigation systems*. Artech House, 2008.
5. G.Welch and G. Bishop. An introduction to the kalman filter. *Department of Computer Science, University of North Carolina at Chapel Hill*, -:–, 2006.
6. InvenSense. *MPU-6000/MPU-6050 Product Specification*, 2011.
7. R. E. Kalman. A new approach to linear filtering and prediction problems. *Transaction of the ASME–Journal of Basic Engineering*, pages 35–45, March 1960.
8. M.G.A. Ruizenaar. Europian patent ep2492637a1. http://www.epo.org/index.html, 2012.
9. William T. Scorse and Agamemnon L. Crassidis. Robust longitudinal and transverse rate gyro bias estimation for precise pitch and roll attitude estimation in highly dynamic operating environments utilizing a two dimensional accelerometer array. In *AIAA Atmospheric Flight Mechanics Conference*, Portland, Oregon, August 2011.
10. E. van der Hall. Driftless gevoeligheids analyse onderzoeks rapport. Technical report, TNO, 2012.
11. N. El-Sheimy Y. Yuksel and A.Noureldin. Error modeling and characterization of environmental effects for low cost inertial mems units. In *Proc. IEEE/ION PLANS, Palm Springs, CA*, 2010.